Available online at www.sciencedirect.com

ScienceDirect

Procedia Structural Integrity 24 (2019) 3–10

Structural Integrity Procedia

www.elsevier.com/locate/procedia

AIAS 2019 International Conference on Stress Analysis

Experimental testing and Numerical modelling of a Kevlar woven – epoxy matrix composite subjected to a punch test

Franco Concli[a], Alvaro Gonzalez-Jimenez[b]*, Andrea Manes[b], Marco Giglio[b]

[a]*Free University of Bolzano/Bozen, piazza Università 1, Bolzano 39100, Italy*
[b]*Politecnico di Milano, Dipartimento di Meccanica, via La Masa 1, Milano 20155, Italy*

Abstract

The paper investigates the penetration mechanics of thick-section composites. For this purpose, a series of quasi-static penetration tests on Kevlar 29 (plane wave) /epoxy panels with a nominal thickness of 6.5 mm (14 layers) were designed and conducted. The experiments were performed at different support spans using a blunt geometry for the punch. During the tests, the punch displacements and the applied force on the punch were measured.
Finite element (FE) models were created to replicate the quasi - static punch test using the LS-DYNA solver and exploiting a material damage model that allows the reproduction of all the different types of failure occurring during the tests (fibre failure, matrix failure, delamination). The focus is placed on the capability of the model to mimic the experimental damage in order to have a reliable virtual tool able to provide, with high accuracy, the penetration mechanisms and the trend of the absorbed energy during the different phases of penetration. The comparison between experimental data and numerical results is discussed.

Keywords: low velocity; CFRP; numerical; LS-DYNA

* Corresponding author. Tel.: +39 02.2399.8668; fax: +39-02 2399 8263.
E-mail address: alvaro.gonzalez@polimi.it

1. Introduction

Whether in the military or in the civil field, composites materials are widely used thanks to both their low density in comparison with traditional materials and their relatively good damage tolerance. Particularly, in the case

2452-3216
10.1016/j.prostr.2020.02.001

of impact events, composites materials are able to partially or completely dissipate the energy of the incoming impactor by means of their specific damage process. However, this damage might be generated by several different failure mechanism including fibre breakage, inter and intralaminar delamination and matrix cracking and their coupling. The understanding of the failure process of composites during impact loading is therefore important in the design process of impact resistant structures.

The ability of composites material to resist high velocity impact loadings is usually measured using the ballistic limit V_{50} performing expensive *in situ* ballistic test. The V_{50} parameter is the cut off velocity below which 50% of the projectiles shot against the target fail to perforate the specimen. In a previous work, Sun *et al* (Sunt & Potti, 1996) stated that the typology of the failure mechanisms observed during a ballistic impact is similar to the mechanisms occurring in a quasi – static punch – shear test. More recently, Gama *et al* (Gama & Gillespie, 2008) studied, in detail, the energies involved in a ballistic impact event on woven glass fibre composites and used the force – displacement curves measured during a punch shear test to obtain the HS-Envelope (*i.e.* the energy that measures the damage of the composite) and the elastic strain energy. With this information, the authors were able to obtain the V_{50} ballistic limit with good agreement. The possibility of ballistically characterizing composites, using punch – shear data, is highly advantageous compared to traditional ballistic tests in which only the initial and final states can be studied. Additionally, a punch - shear test is less complex and expensive than a ballistic impact, and the implementation of a numerical finite element virtual test might further reduce the efforts enabling a selection of the most promising composite with a reduced quantity of experimental tests. This approach was followed by Xiao *et al* (Xiao, Gama, & Gillespie, 2007) that use a span ratio (SPR) (*i.e.* the ratio between the punch diameter, D_p and the support central hole diameter, D_s) of 0. The authors performed a numerical punch – shear test on S2-glass/epoxy composites using the software LS-DYNA and exploiting the material model 162 which presents a linear elastic loading phase with a negative exponential strain softening behaviour. This material model can consider several failure modes including delamination and fibre crush. They obtained good agreement both in the reproduction of the load – displacement curve and in the capturing of the shear plug formation.

In the literature, punch – shear studies are generally focused on glass fibre composites. However, Kevlar composites have a potentially different damage behaviour due to their thermoplastic nature. In the present study, an experimental punch – shear test of woven Kevlar 29/epoxy composites with a SPR of 2, 4 and 8 is tested and analysed. Subsequently, the numerical model of all the experimental tests is implemented on the software LS-DYNA. For this purpose, the material model 58 based on the Matzenmiller strain softening criteria (Matzenmiller, Lubliner, & Taylor, 1995) is employed for the simulation the intralaminar properties of the composite. Material Model 58 is intended for the use with shell or thick shell elements to simulate composite tape laminates and woven fabrics. Through the appropriate selection of the specific parameters, plastic-like behaviour can be incorporated in the model and premature element failure is avoided. For the analysis of the interlaminar behaviour, a penalty – based stiffness method with the possibility of debonding is used.

2. Experimental set-up and specimen configuration

The specimens were built following an autoclave process. They were manufactured using plain weave Saatilar Kevlar 29 fibres and Microtex E9 matrix series epoxy resin. The dimensions of the specimen were 150x150mm with central eight holes positioned at a distance of 10 mm from the border and distanced 65mm from one another. Each specimen was composed of 14 layers with an approximate layer thickness of 0.46mm resulting in a total thickness (H_c) of 6.5 mm.

The experimental set-up was composed of a square steel support plate for each SPR, an identical steel cover plate for all the tests and a flat – nose blunt steel punch impactor with a 12.7mm diameter. The specimens were fixed between the support and the cover plate by means of 8 M8 bolts. A diagram of the punch-shear set-up is shown in Figure 1.

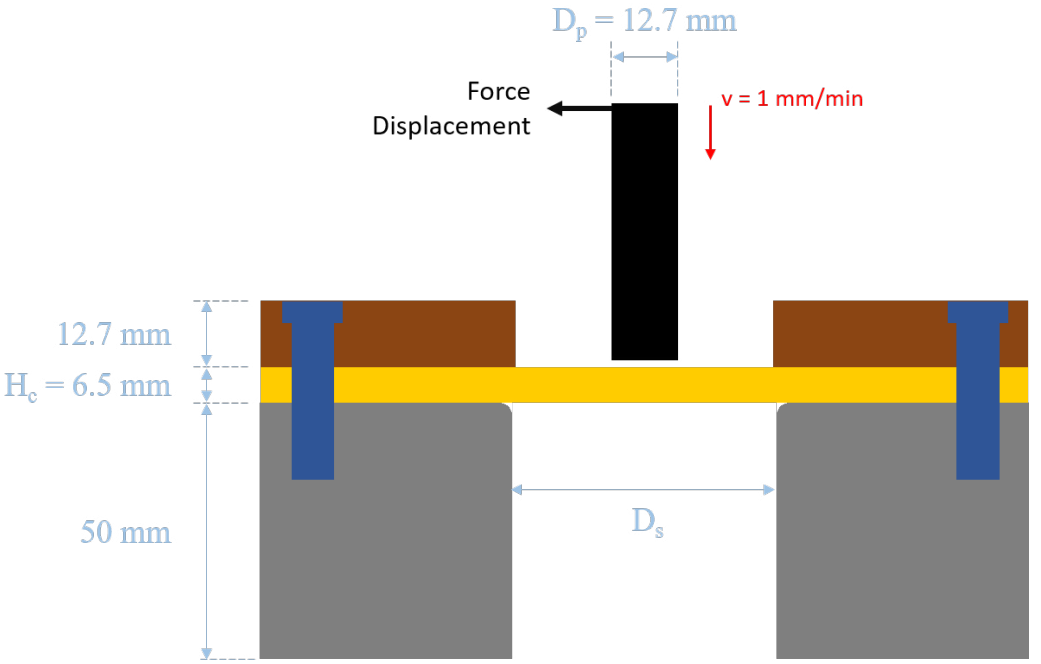

Figure 1 Diagram of the experimental punch-shear set-up: the punch in black, the bolts in blue, the cover plate in brown, support in grey, the specimen in yellow.

Both the support and the cover plates have a quadratic form of 150x150mm with 8 centered holes distanced 10 mm from the borders to match them with the perforated specimen. A centered circular hole was also perforated into both the support and cover plate with the dimensions of 25.4mm, 50.8mm and 101.6mm in order to match the SPR of 2, 4 and 8 respectively.

The test apparatus was designed to fit the MTS universal testing machine available at the Free University of Bolzano. The reaction force of the punch was measured using a load cell sensor while the displacement was measured with the cross – head of the testing machine and the velocity was set to 1mm/min.

3. Numerical modelling

Only one quarter of the whole set-up was simulated to increase the calculation efficiency, and the proper symmetry conditions were applied to the composite. The boundary conditions are believed to affect the results of the numerical simulation and therefore the bolted union of the composite with the cover/support plate were modelled. The bolts, support plate, cover plate and punch were regarded as rigid materials with no possible deformation allowed. This renders the models more computationally efficient. An overall view of the model implemented is shown in Figure 2.

The material parameters of the lamina, used in the current simulation, and their source are listed in Table 1.

Table 1 Mechanical parameters for the material used

Intralaminar properties			
Variable	Acronym	Value	Source
Density	ρ	1.025 [g/cm^3]	Experimental
Modulus of elasticity in direction 1	E_1	10030 [MPa]	Experimental
Modulus of elasticity in direction 2	E_2	10030 [MPa]	Experimental
Modulus of elasticity in direction 3	E_3	6000 [MPa]	(Bresciani *et al* 2016)
Shear modulus in direction 12	G_{12}	5510 [MPa]	(Berk *et a*l 2017)
Shear modulus in direction 13	G_{13}	3300 [MPa]	(Berk *et al*., 2017)
Shear modulus in direction 23	G_{23}	3300 [MPa]	(Berk *et a*l., 2017)
Poisson ratio in direction 12	ν_{12}	0.21 [-]	Experimental
Poisson ratio in direction 13	ν_{13}	0.33 [-]	(Bresciani *et al*., 2016)
Poisson ratio in direction 23	ν_{23}	0.33 [-]	(Bresciani *et al*., 2016)
Tensile strength in direction 1	X_t	405 [MPa]	Experimental
Tensile strength in direction 2	Y_t	185 [MPa]	(Bresciani *et al*., 2016)
Compressive strength in direction 1	X_c	405 [MPa]	Experimental
Compressive strength in direction 2	Y_c	185 [MPa]	(Bresciani *et al*., 2016)
Shear strength in direction 12	S_{12}	66 [MPa]	(Berk *et al*., 2017)
Shear strength in direction 13	S_{13}	40 [MPa]	(Berk *et al*., 2017)
Shear strength in direction 23	S_{23}	40 [MPa]	(Berk *et al*., 2017)
Interlaminar properties			
Mode I strength	NFLS	34.60 [MPa]	(Gower, Cronin, & Plumtree, 2008)
Mode II strength	SFLS	9.00 [MPa]	(Gower *et al*., 2008)

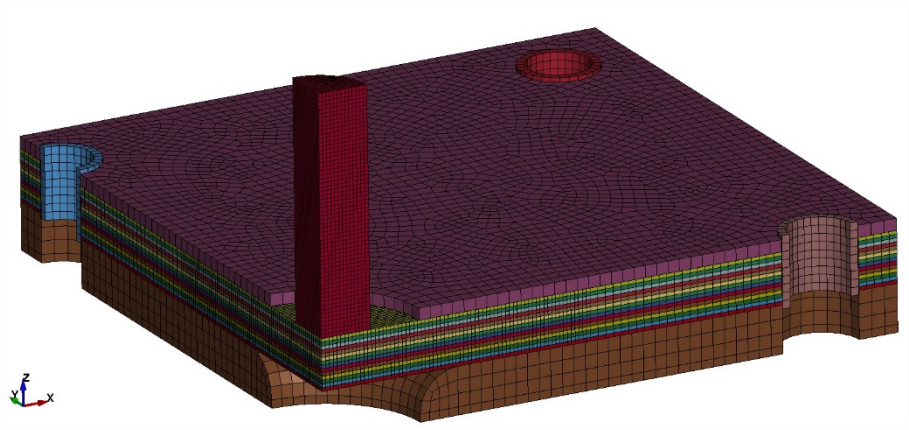

Figure 2 Numerical model representation

A general contact AUTOMATIC_SURFACE_TO_SURFACE in LS-DYNA was implemented between the support plate and the composites, between the cover plate and the composites and between the bolts and the composite. A friction coefficient of 0.4 was considered for all these three contacts. Due to the fact that the elements in direct contact with the punch might be removed during the simulation creating a new contact surface, the contact formulation ERODING_SURFACE_TO_SURFACE was utilized between the punch and the whole composite. Also, a friction coefficient of 0.4 was set between these two parts. For the case of the punch, only the displacement on the vertical direction was allowed and all other rotations/displacements were prevented. For the case of the plates and the bolts all

degrees of freedom were fixed.

Regarding the intralaminar behaviour of the composite, the material model 58 (MAT58) of LS-DYNA was chosen for two reason: it considers several failure modes with a reduced number of input parameters and it presents a constitutive law based on the Weibull distribution. This distribution is obtained from a statistical analysis of the failure probability of a bundle of ceramic fibres (Matzenmiller et al., 1995). This distribution dictates the constitutive behaviour of MAT58: from the origin to the maximum value the loading behaviour is represented and from the maximum value on, the strain softening behaviuor is defined. Additionally, the post - damage behaviour can be controlled by the definition of a residual strength through the parameter SLIM*X*. This parameter represents a percentage of the failure onset strength of the composite, when the failure onset defined by the Hashin equation is met (*i.e.* failure onset) (Hashin, 1980) the stress of the element is reduced to a value equal to SLIM*X* multiplied by the material strength. This stress is kept constant until the element is canceled. For the current case, a threshold of the equivalent Von Mises strain was set above which the element was canceled.

A tiebreak contact algorithm was employed to acknowledge the interlaminar damage of the composite. This formulation considers the measurement of two points which are initially in contact and set a limit distance which generates the breakage of the contact generating two new surfaces (Dogan, Hadavinia, Donchev, & Bhonge, 2012). In particular, the penalty-based stiffness methodology was implemented in the present model. This contact considers that two nodes are joint by a spring which stiffness will provide the force generated by the contact. This contact is called AUTOMATIC_SURFACE_TO_SURFACE_TIEBREAK in the contact library of LS-DYNA.

Composite structures are extensively used in several industrial fields such as civil aviation or sports. This creates the need to implement time efficient numerical models with a low computational cost. Therefore, a non – uniform mesh was used for the composite layer and in the area of interest, a regular mesh with a maximum dimension of 0.5mm was employed. A coarser mesh of about 1mm was utilized in the composites zones which are far away from the impact area. The formulation of the elements selected was continuum shell of thick shell elements keeping in mind the time efficiency of the model. Particularly, thin – thick shell identified as ELFORM 1 in LS-DYNA was employed. This element type is based on the Reissner – Mindlin theory and has one integration point on the in – plane direction while 3 integration points in the thickness direction were defined.

4. Results and discussion

This section contains the experimentally obtained results and their comparison and confrontation with the numerically obtained data.

1.1. Experimental results

The experimental results for the SPR of 2, 4 and 8 are shown in Figure 3.

The energy categorization observed in (Gama & Gillespie, 2008) can be perfectly distinguished for all the three SPR. They present a bilinear behaviour as observed in (Xiao et al., 2007) for a thick composite (i.e. $D_P D_S/H_c^2 < 100$). The points of interest were marked on the SPR = 2 curve. The description of the different portion of the load – displacement curves are:

- from the beginning of the curve to point A, a linear – elastic part without the presence of damage can be defined. This part is present in the three curves and the slope of this elastic part is decreasing with an increasing SPR. Logically, this is created by the larger gap between the force application area and the support;
- from points A to B the first significant force drop is visible. This first damage is believed to be caused by matrix cracking;
- from points B to C a second approximately linear part can be defined in which delamination starts to form and propagate. Furthermore, at a displacement of 5.1mm the first large force drop occurs which might correspond with the actual delamination initiation. Damage is mainly generated in the last portion of this phase since larger force oscillations are visible. For force level near the peak force, probably and besides the delamination

propagation, the shear plug of the starts to form due to high compression shear around the punch edge; from C to D the shear plug is completely formed;
- from D to E the formed shear plug slides through the composites and further fiber breakage is generated in the back face. This additional fiber breakage might generate the slight oscillations observed;
- from E and beyond a plateau like trend is reached at a residual value of force. This is generated by the friction between the punch and the broken walls of the composite.

When the span ratio is increased, the small oscillations in the first part of the equivalent C – D portion are increased. For larger SPR, the bending deformation of the composites is increased creating a higher shear state of stresses on the composite interphases which generated a larger delaminated area in Mode II resulting in these small oscillations.

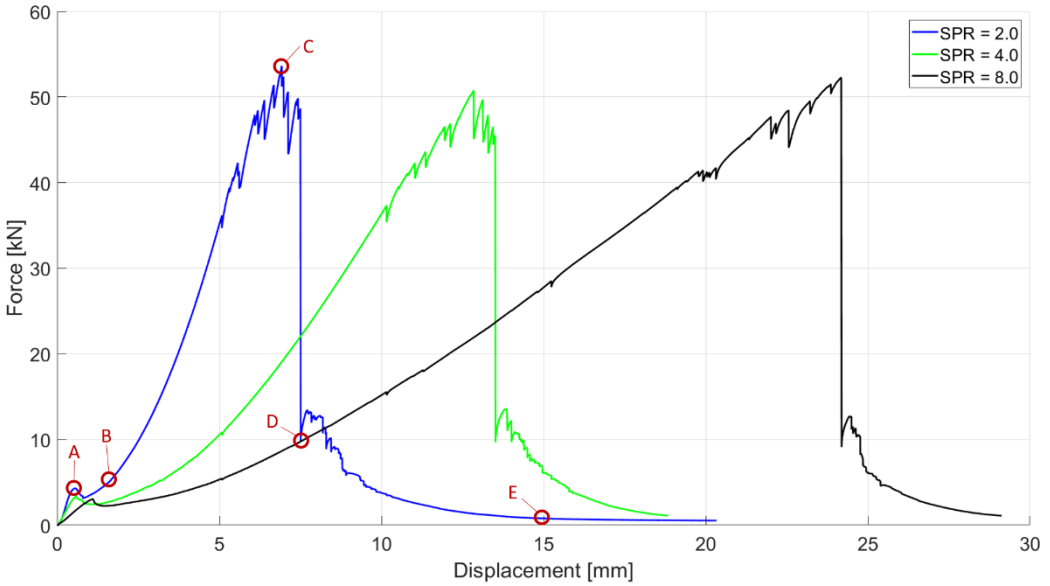

Figure 3 Experimental results for all three SPR with the five points of interest A, B, C, D and E marked in red.

1.2. Numerical comparison

A parametric analysis for SLIMT, ERODS was performed before the implementation of the final model. The experimental definition of these parameters is often impossible, and it requires a numerical calibration process. SLIMT and ERODS represent respectively, the residual strength in direction 1 under tension and the equivalent Von Mises strain for the element deletion. After the analysis, the best numerical – experimental agreement was found for SLIMT of 0.8 (i.e. 80% of the material strength is considered once the element reaches the failure onset) and an ERODS of 1.5.

In addition, two models were considered for a sensitivity analysis of the boundary condition. In the first model all the nodes belonging to the inner surface of the bolt holes were fixed and in the second model the bolts were modelled and consider as rigid bodies with a proper contact among the rigid bolts and the composite. The second model provides a more realistic view of the real experimental set-up since the section of the composite in contact with the bolt might suffer from a section change or, in other words, not all the nodes remain attached to the bolt during the test. Additionally, it was verified that the bolts being rigid bodies caused no significant increment of the computational time. Consequently, and as shown in Figure 2 the bolts were considered as rigid bodies for the final simulation.

The numerical – experimental data comparison of all three SPR is shown in Figure 4. The dashed line represents the numerical and the solid line the experimental results.

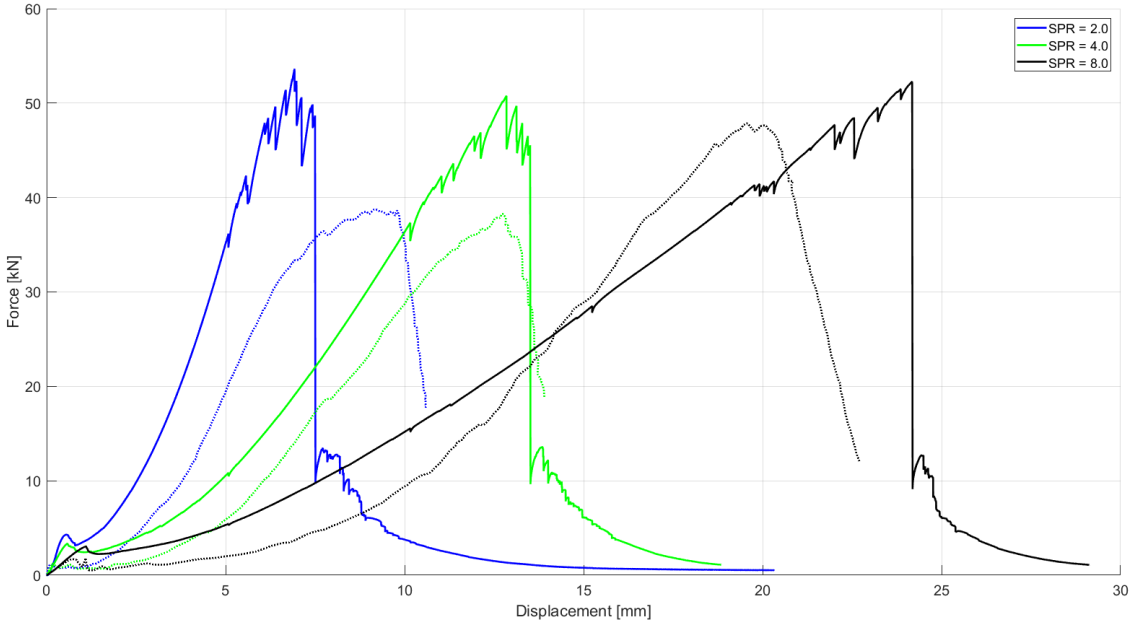

Figure 4 Numerical (dashed line) – experimental (solid line) data comparison

The agreement between the numerical and the experimental data increased with the augmentation of the SPR. It appears that after the occurrence of the first damage (i.e. the first appreciable force drop) the compliance of the material is not well captured. The disagreement initially appears in the A – B phase which is dominated by the matrix cracking failure and in which the correct transmission of load in the out – of – plane direction is important. Therefore, the numerical – experimental mismatch is believed to be generated by two facts: the thick shell elements formulation used might not transmit properly the through – the – thickness load and the material model 58 is unable to correctly represent the failure process of the matrix under compression. It is worth mentioning that the model presented above is a first approximation of the punch – shear problem. In future works, solid elements along with more complete material models such as the material model 162 of LS-DYNA will be studied in depth.

5. Conclusions

In the present work, the analysis of a quasi – static punch – shear test was performed for three SPR of 2, 4 and 8. These tests were performed on thick woven Kevlar/epoxy composites. The damage mechanisms were distinguishable on the force – displacement curves and the mechanisms were fairly similar to other punch – shear studies present in the literature.

Additionally, three models for the three SPR studied were implemented in the software LS-DYNA. The material model 58 based on the Hashin failure onset criteria with the Matzenmiller damage progression formulation was used for the simulation of the intralaminar behaviour, whereas the debonding among two initially attached layer was reproduced employing a tiebreak contact formulation consisting of a penalty-based stiffness method with a failure criterion based on the relative node displacement. While the SPR of 8 was correctly modeled by the material model 58 only a discrete agreement with experimental data was obtained for the SPR of 2 and 4. This incomplete capacity of the material model 58 to capture the failure mechanism of composites under punch – shear test is most likely linked to its incapacity to consider out – of – plane failure process.

References

Berk, B., Karakuzu, R., & Toksoy, A. K. (2017). An experimental and numerical investigation on ballistic performance of advanced composites. *Journal of Composite Materials*, *51*(25), 3467–3480. https://doi.org/10.1177/0021998317691810

Bresciani, L. M., Manes, A., Ruggiero, A., Iannitti, G., & Giglio, M. (2016). Experimental tests and numerical modelling of ballistic impacts against Kevlar 29 plain-woven fabrics with an epoxy matrix: Macro-homogeneous and Meso-heterogeneous approaches. *Composites Part B: Engineering*, *88*, 114–130. https://doi.org/10.1016/j.compositesb.2015.10.039

Dogan, F., Hadavinia, H., Donchev, T., & Bhonge, P. S. (2012). Delamination of impacted composite structures by cohesive zone interface elements and tiebreak contact. *Central European Journal of Engineering*, *2*(4), 612–626. https://doi.org/10.2478/s13531-012-0018-0

Gama, B. A., & Gillespie, J. W. (2008). Punch shear based penetration model of ballistic impact of thick-section composites. *Composite Structures*, *86*(4), 356–369. https://doi.org/10.1016/j.compstruct.2007.11.001

Gower, H. L., Cronin, D. S., & Plumtree, A. (2008). Ballistic impact response of laminated composite panels. *International Journal of Impact Engineering*, *35*(9), 1000–1008. https://doi.org/10.1016/j.ijimpeng.2007.07.007

Hashin, Z. (1980). Failure Criteria for Unidirectional Fiber Composites. *Journal of Applied Mechanics*, *47*(2), 329. https://doi.org/10.1115/1.3153664

Matzenmiller, A., Lubliner, J., & Taylor, R. L. (1995). A constitutive model for anisotropic damage in fiber-composites. *Mechanics of Materials*, *20*(2), 125–152. https://doi.org/10.1016/0167-6636(94)00053-0

Sunt, C. T., & Potti, S. V. (1996). *Velocities of Thick Composite Laminates Subjected To High Velocity Impact*. *18*(3), 339–353.

Xiao, J. R., Gama, B. A., & Gillespie, J. W. (2007). Progressive damage and delamination in plain weave S-2 glass/SC-15 composites under quasi-static punch-shear loading. *Composite Structures*, *78*(2), 182–196. https://doi.org/10.1016/j.compstruct.2005.09.001